Available online at www.sciencedirect.com

SCIENCE DIRECT®

International Journal of Psychophysiology 53 (2004) 75–90

INTERNATIONAL JOURNAL OF PSYCHOPHYSIOLOGY

www.elsevier.com/locate/ijpsycho

Linkage and linkage disequilibrium of evoked EEG oscillations with *CHRM2* receptor gene polymorphisms: implications for human brain dynamics and cognition

Kevin A. Jones[a], Bernice Porjesz[a,*], Laura Almasy[b], Laura Bierut[c], Alison Goate[c], Jen C. Wang[c], Danielle M. Dick[c], Anthony Hinrichs[c], Jennifer Kwon[c], John P. Rice[c], John Rohrbaugh[c], Heather Stock[c], William Wu[c], Lance O. Bauer[d], David B. Chorlian[a], Raymond R. Crowe[e], Howard J. Edenberg[f], Tatiana Foroud[f], Victor Hesselbrock[d], Samuel Kuperman[e], John Nurnberger Jr[f], Sean J. O'Connor[f], Marc A. Schuckit[g], Arthur T. Stimus[a], Jay A. Tischfield[h], Theodore Reich[c], Henri Begleiter[a]

[a] *Department of Psychiatry, Neurodynamics Laboratory, SUNY Health Science Center, 450 Clarkson Avenue, Box 1203, Brooklyn, NY 11203, USA*
[b] *Southwest Foundation for Biomedical Research, San Antonio, TX, USA*
[c] *Washington University School of Medicine, St. Louis, MO, USA*
[d] *University of Connecticut, Farmington, CT, USA*
[e] *University of Iowa, Psychiatry Research, Iowa City, IA, USA*
[f] *Indiana University School of Medicine, Indianapolis, IN, USA*
[g] *University of California, San Diego, CA, USA*
[h] *Rutgers University, Piscataway, NJ, USA*

Received 14 November 2003; received in revised form 10 February 2004; accepted 11 February 2004

Abstract

Event-related oscillations (ERO) offer an alternative theoretical and methodological approach to the analysis of event-related EEG responses. The P300 event-related potential (ERP) is elicited through the superposition of the delta (1–3 Hz) and theta (3–7 Hz) band oscillatory responses. The cholinergic neurotransmitter system has a key function in modulating excitatory post-synaptic potentials caused by glutamate, and therefore influences P300 generation and the underlying oscillatory responses. Here we report significant linkage and linkage disequilibrium between target case frontal theta band, visual evoked brain oscillations and a single nucleotide polymorphism (SNP) from the cholinergic muscarinic receptor gene (*CHRM2*) on chromosome 7. We also demonstrate significant linkage disequilibrium between *CHRM2* SNPs and target case parietal delta band visual evoked oscillations (LD $P<0.001$). These findings were not observed for the equivalent non-target case data, suggesting a role for the *CHRM2* gene in higher cognitive processing in humans.

Keywords: Event-related oscillations; P300; Delta; Theta; Cholinergic muscarinic receptors; *CHRM2*; Linkage disequilibrium

* Corresponding author. Tel.: +1-718-270-2024; fax: +1-718-270-4081.
E-mail address: bp@cns.hscbklyn.edu (B. Porjesz).

0167-8760/$ - see front matter © 2004 Elsevier B.V. All rights reserved.
doi:10.1016/j.ijpsycho.2004.02.004

1. Introduction

Neurophysiological features extracted from EEG data, such as event-related brain potentials (ERP's), have provided a non-invasive and reliable mechanism to study both animal and human cognitive function (Sutton et al., 1965; Donchin, 1979; Polich and Kok, 1995). The proven functional significance of EEG has sanctioned its use as a phenotype of cognition and a valuable tool for the understanding of some complex genetic disorders. These phenotypic measures are also of great consequence because they represent traits more proximal to gene function than either diagnostic or traditional cognitive measures. Recent work has proven that the genetic influence on evoked potentials is significant. In particular, twin studies have indicated strong evidence for the high heritability of the P300 component amplitude (O'Connor et al., 1994; Katsanis et al., 1997; Van Beijsterveldt et al., 1998). A P300 amplitude heritability estimate of 60% has been established through a meta-analysis of five P300 twin studies (Van Beijsterveldt and Van Baal, 2002). Similar P300 ERP amplitude heritability values were obtained for parietal electrodes in 100 families (Almasy et al., 1999).

The P300 component of the human ERP was first observed in 1965 (Sutton et al., 1965) and can be defined as the third positive EEG deflection which initializes at approximately 300 ms (depending on modality) following the presentation of an infrequent task-related event. Typically the P300 wave is evoked using a task known as the oddball paradigm, during which a series of one type of stimulus (visual, auditory or olfactory) is presented to the subject. An infrequent stimulus requiring a motor response, such as pressing a button or a mental count, is used to elicit the P300 target event. Studies using invasive methods have identified the temporo-parietal junction and neighboring parietal and temporal neo-cortical regions as important P300 generator sites (Hruby and Marsalek, 2003). Intracranial recording methods indicate that deeper structures, such as the hippocampus, parahippocampal gyrus, amygdala, and thalamus, have an important role in P300 generation (Halgren et al., 1980; Okada et al., 1983; Rogers et al., 1993).

ERP events occurring prior to the P300 event, such as the N100 and P200, are typically studied to understand sensory cortex projection pathways, selective attention, early object recognition, and processing perceptual mismatch (Mangun et al., 1998). Later ERP components have been associated with higher cognitive processes such as object recognition, motor planning, working memory, memory rehearsal, error processing, and inhibitory executive control (Donchin and Coles, 1988; Ruchkin et al., 1995; Geffen et al., 1997). Individuals with neurological and psychiatric disorders have been shown to exhibit changes in the amplitude and latency of the P300 component. For example, a reduced P300 amplitude in patients with schizophrenia has been repeatedly established (Roth et al., 1981; Frodl-Bauch et al., 1999b). Thus, the P300 wave has fundamental clinical relevance.

Evidence suggests that ERP components may be generated in part through stimulus-induced changes of ongoing brain dynamics (Makeig et al., 2002) rather than the traditional view of generation through transient, non-rhythmic, stimulus evoked brain events. Traditional methodology assumes that the averaging of the event-related EEG data reveals the fixed latency, fixed polarity sensory evoked ERP components while eliminating the non-stimulus related background oscillatory EEG activity. Theories of event-related brain dynamics, however, suggest that the ERP components arise from changes in the dynamics of ongoing neural synchrony generating the scalp EEG (Basar, 1980; Makeig et al., 2002), and in relation to sensory and cognitive processes (Schurmann et al., 1995; Yordanova and Kolev, 1998; Karakas et al., 2000a,b; Schurmann et al., 2001). These theories support the notion that brain events are not purely amplitude modulated, but contain a significant portion of phase modulation. Evoked EEG rhythms, or event-related oscillations (ERO), may be quantified by examination of the constituent frequency components of event-related potential data. Typically, the data are segregated along the lines of the traditional EEG frequency bands: delta (1.0–2.5 Hz); theta (3.0–7.0 Hz); alpha-1 (7.5–9.0 Hz); alpha-2 (9.5–12.0 Hz); beta-1 (12.5–16.0 Hz); beta-2 (16.5–20.0 Hz); beta-3 (20.5–29.0 Hz); and gamma (>29.0 Hz). Such data have been extensively used to study cognitive processing (Klimesch et al., 1997; Schurmann et al., 1997; Basar et al., 2000, 2001; Klimesch et al.,

2001). The use of event-related brain oscillations is well suited to the study of this new field of 'event-related brain dynamics'. Different frequency rhythms of oscillatory responses have been correlated with various cognitive processes. For instance, evoked delta oscillations are attributed to signal evaluation and decision making (Basar et al., 1999, 2001). Evoked theta oscillations are correlated with attention, conscious awareness, episodic retrieval, and recognition memory (Doppelmayr et al., 1998; Klimesch et al., 2001). The higher frequency evoked gamma oscillations are involved in visual perception and cognitive integrative function (Schurmann et al., 1997; Basar et al., 2001).

Given the importance of the evoked response P300 oscillations in the study of cognitive processes in humans, and the compelling evidence indicating that these neuroelectric features are substantially under genetic control, identifying genes which control or influence the P300 appears possible. In this report, we present the results of genetic analyses of electrophysiological features derived from the visual P300 event-related oscillations recorded from individuals as part of the Collaborative Study on the Genetics of Alcoholism (COGA). Previous analysis of the same COGA dataset has yielded significant evidence of linkage and linkage disequilibrium in a region of chromosome 4 centered on the GABA(A) receptor gene cluster for resting EEG beta band (13–28 Hz) power spectral data (Porjesz et al., 2002; Ghosh et al., 2003). Significantly, it has been shown that alcoholics and offspring of alcoholics at risk have increased resting EEG beta power, suggesting that such data may act as an endophenotype of alcoholism (Rangaswamy et al., 2002, 2004). Here we focus our attention on the visual oddball paradigm delta and theta frequency band evoked oscillations since it is known that these frequencies are the primary constituents of the interesting cognitive P300 evoked component (Stampfer and Basar, 1985; Demilrap et al., 1999). Initial results from a genome-wide linkage analysis scan provided evidence of linkage to the region containing the *CHRM2* gene, making it an excellent candidate gene influencing the phenotype. Subsequent linkage disequilibrium analysis with single nucleotide polymorphisms, within and flanking the *CHRM2* gene, provided strong evidence that the quantitative phenotypes are influenced by *CHRM2* or by a nearby genetic variant trait that is in linkage disequilibrium (LD) with the *CHRM2* gene. These results lend support for a role for the *CHRM2* gene in human brain dynamics and cognitive processing, and demonstrate the utility of genetics in the area of neuroscience.

2. Materials and methods

2.1. Subjects

Subjects included in this study were recruited and tested as part of the multisite Collaborative Study on the Genetics of Alcoholism (COGA), a large national study implemented with the purpose of identifying genetic loci linked with the predisposition to develop alcoholism. Data from six COGA sites were included in the analysis: SUNY Downstate Medical Center, New York; University of Connecticut Health Science Center; Indiana University School of Medicine; University of Iowa School of Medicine; University of California School of Medicine, San Diego; and Washington University School of Medicine, St Louis. Ascertainment and assessment procedures have been described elsewhere (Begleiter et al., 1995).

The total sample included in this genetic analysis consisted of 1337 individuals drawn from 253 families and ranging in age from 16 to 75 years. A Caucasian-only sub-sample comprising of 1067 individuals from 210 families was used in the linkage disequilibrium analysis. Laboratory and data collection procedures were identical at each of the sites (Begleiter et al., 1998). Blood was obtained from subjects for DNA extraction and estimation of microsatellite marker data and single nucleotide polymorphisms (SNPs) for use in general pedigree linkage and linkage disequilibrium analysis. Genotyping was performed at Washington University and Indiana University.

2.2. EEG data recording

Electrophysiological recordings were carried out using a fitted electrode cap containing 19 channels arranged according to the international 10–20 system (FP1, FP2, F7, F3, FZ, F4, F8, T7, C3, CZ, C4, T8,

P7, P3, PZ, P4, P8, O1, and O2); see Fig. 1. An electrode placed on the subject's nose served as the reference and one on the forehead as a ground. Electrical activity was amplified 10 K (Sensorium EPA-2 Electrophysiology Amplifiers) and recorded over a bandwidth of 0.02–50.0 Hz at a sampling rate of 256.0 Hz. The visual oddball paradigm employed by COGA was described in a study on intersite data collection consistency (Cohen et al., 1994). Three types of visual stimuli were presented: target (the letter X), non-target (squares), and novel (a different colored geometric figure on each trial). The probabilities of occurrence of the trials were 0.125 for the target trials, 0.75 for non-target trials, and 0.125 for novel trials. Each stimulus shape subtended a visual angle of 2.5°. Stimulus duration was 60 ms, and the interstimulus interval was 1.6 s. Subjects were requested to respond to the target stimulus by pressing a button with the left or right index finger. Response speed was emphasized, but not at the cost of accuracy. Trials with baseline corrected amplitudes greater than 73.3 μV were marked as artifact contaminated. The experiment terminated automatically when a minimum of 25 target stimuli, 150 non-target stimuli, and 25 novel stimuli artifact free trials had been acquired. Common stimulus single trial data from each subject were processed for further genetic analysis using time-frequency representations (see below).

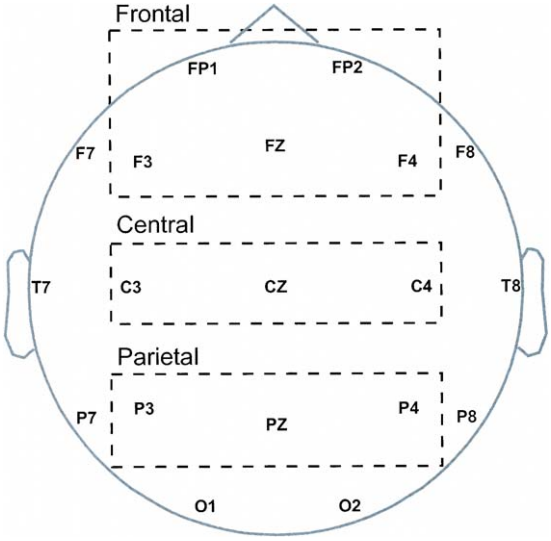

Fig. 1. Aerial view of the scalp with the nose up (top) designating the positions of the electrodes in the 10–20 international system. F, frontal; C, central; P, parietal; O, occipital; and T, temporal. Odd numbers indicate leads on the left side of the head, even numbers indicate leads on the right side of the head and Z indicates zero or midline. For the genetic analysis, measures on individual leads were averaged into the three scalp regions indicated by the dashed rectangles (frontal, central and parietal).

2.3. ERO energy estimation

To obtain reliable estimates of localized power of non-stationary evoked potential time series, we employed a recently developed time-frequency representation method: the S-transform (Stockwell et al., 1996). The S-transform is a generalization of the Gabor transform (Gabor, 1946) and an extension to the wavelet transform. The S-transform generates a time-frequency representation (TFR) of a signal by integrating the signal at each time point with a series of windowed harmonics of various frequencies as follows:

$$ST(f,\tau) = \int_{-\infty}^{\infty} h(t)\frac{|f|}{\sqrt{2\pi}} e^{-\frac{(\tau-t)^2 f^2}{2}} e^{i2\pi f t} dt$$

where $h(t)$ is the signal, f is frequency, τ is a translation parameter, the first exponential is the window function, and the second exponential is the harmonic function. The S-transform TFR is computed by shifting the window function down the signal in time by τ across a range of frequencies. The window function is Gaussian with $1/f^2$ variance and scales in width according to the examined frequency. This inverse dependence of the width of the Gaussian window with frequency provides the frequency-dependent resolution. The Hilbert transform (amplitude envelope) of the complex-valued S-transform TFR is calculated by taking the absolute value $ST(f,\tau)$.

The electrophysiological phenotypic data used in the analysis were derived from the single trial visual oddball event-related data for both target and non-target cases. The amplitude envelope of the S-transform TFR were averaged across single trials, per individual, to obtain an estimate of event-related total energy response (stimulus onset phase locked plus non-phase locked oscillations). The total energy response enhances events that occur in a similar time range as related to the stimulus onset, and irrespective of their phase relations. Mean values were calculated

from the TFR for use as phenotypes within time-frequency regions of interest (TFROI's) (Lachaux et al., 2003) specified by frequency band ranges and time intervals. The data were further aggregated to form the three scalp regions illustrated in Fig. 1: frontal (channels FP1, FP2, F3, FZ and F4); central (channels C3, CZ and C4); and parietal (channels P3, PZ and P4). This study focused on evoked oscillation TFROI corresponding to the delta (1.0–2.5 Hz) and theta (3.0–7.5 Hz) frequency bands and the P300 time window range (determined from grand average data to be from 300 to 700 ms).

2.4. Genotyping

Publicly available databases (http://www.ncbi.nlm.nih.gov/SNP/, http://www.ncbi.nim.nih.giv/LocusLink/refseq.html) were used to identify single nucleotide polymorphisms (SNPs) within and flanking the *CHRM2* gene. PCR primers were selected using the MacVector 6.5.3 program (Oxford Molecular Group, Inc.) to give 200–500 bp genomic fragments containing the SNP. All of the SNP genotyping was performed using a Pyrosequencing method (Pyrosequencing AB). Standard PCR procedures were followed to generate PCR products. The sequence of the PCR product was entered into the Pyrosequencing Primer Design program (www.pyrosequencing.com) to select sequencing primers for the SNP assay.

2.5. Linkage and linkage disequilibrium analysis

Genome-wide linkage analyses search for patterns of DNA sharing among family members that match the patterns of correlation in phenotype among family members. In particular, the variance component analyses used in this study model the correlation in phenotype among relatives as a function of identity-by-descent (i.b.d.) allele sharing in the region of a genotyped marker and residual sharing elsewhere at unspecified regions of the genome. The expected residual sharing in unspecified areas is quantified by the kinship coefficient, a measure of relatedness among family members. Identity-by-descent allele sharing concerns DNA sharing at a particular chromosomal region and is a measure of whether two relatives inherited their DNA in that region from a common ancestor. In linkage analyses, it is the common ancestral origin of the DNA segment that matters, rather than its content. Two family members may have the same genotype, but if they inherited these alleles from different ancestors, they would not be considered identical-by-descent. Thus, linkage analyses trace the co-segregation of phenotype and genotype through the family tree and test whether a gene, or quantitative trait locus (QTL), influencing the phenotype is linked to the genotyped marker locus. The traditional measure of the strength of a linkage signal is the log-odds (LOD) score. LOD scores are on a logarithmic scale. A LOD score of 3 represents 1000 times more support for the hypothesis of linkage vs. no linkage and is generally accepted as the threshold for genome-wide significance, taking into account the multiple testing inherent in a genome-wide screen.

In contrast to linkage analyses, linkage disequilibrium (LD) or association analyses directly test for correlations between phenotype and genotype and are based on identity-by-state (i.b.s.) allele sharing. That is, in linkage disequilibrium analyses it is the form of the genotype that is important rather than its ancestral origin, and any individuals with the same genotype are grouped together. Whereas microsatellite markers are generally used for linkage analyses, single nucleotide polymorphisms (SNPs) are frequently used for linkage disequilibrium analyses. Microsatellite markers are variations in the number of times a particular sequence, usually two to four nucleotides in length, is repeated. They have many alleles (polymorphic), which are beneficial for linkage analyses as they facilitate distinguishing between the contributions of different ancestors. In contrast, SNPs generally have only two alleles. However, SNPs occur more frequently in the genome and lend themselves more easily to a simple association test as only three genotypes are possible with two alleles at the marker. In these particular analyses, we test whether the phenotypic mean differs between individuals with different genotypes with significance assessed by comparing the likelihood of a model with genotype-specific trait means to that of a model with equal means for all genotypes.

The quantitative evoked oscillation phenotypes were used in a variance component linkage analysis implemented with SOLAR (Almasy and Blangero, 1998). The appropriate variance–covariance matrix

for a pedigree depends on the predicted proportion of genes shared i.b.d. at a hypothesized quantitative trait locus, QTL; this proportion depends in turn on the proportion shared i.b.d. at genotyped microsatellite markers and on the type of relative pair. Maximum likelihood estimates for the variance component parameters were obtained, and a LOD score was computed as log10 of the likelihood ratio comparing two models: a model where the additive genetic variance $\sigma^2 a$ for the QTL is estimated vs. a model where $\sigma^2 a$ is constrained to be zero (no linkage). Variance component linkage analyses were carried out at 1 cM intervals across all chromosomes. The analyses were performed using the *t*-distribution option of SOLAR, rather than the multivariate normal distribution, since the *t*-distribution is less susceptible to distributional violations caused by slight kurtosis observed in the phenotype data (Blangero et al., 2001). Gender, gender-specific age, age, and age-squared data were incorporated in the analysis as covariates and retained when a likelihood ratio test was deemed significant ($P<0.1$) for these covariates. The initial genome-wide linkage scan of delta and theta band evoked oscillation phenotypes was performed employing the entire COGA dataset available with electrophysiological data (1337 individuals from 253 families).

Measured covariate effects such as age, gender gender-specific age, and age-squared, are modeled using SOLAR as fixed effects on the phenotype trait mean; variance component effects, such as quantitative trait loci, the residual additive genetic component, and the residual environment, are modeled as random effects. Variance component effects, therefore account for the variance in the data, which is not absorbed by the trait mean and the specified covariates (Almasy and Blangero, 2003). Within this modeling structure, a test for linkage disequilibrium between a SNP and a QTL can be achieved by incorporation of the mean effects model as a measured covariate (Boerwinkle et al., 1986). Both additive and dominant models may be tested as measured genotype covariates in a linkage disequilibrium analysis. The additive measured genotype model assumes that each dose of the variant allele has an equal effect on a trait mean and places the heterozygote mean halfway between the homozygotes, thereby allowing a test of the trait mean variation with genotype. To allow SNP variant models to be included as fixed effect covariates in the variance component analysis, the additive model is coded as −1 for AA SNP genotypes, 0 for Aa SNP genotypes, and 1 for aa SNP genotypes. The dominant model allows a measure of how the trait mean for heterozygotes varies from the homozygote halfway point; this model is coded as 1 for AA and aa SNP genotypes, and 0 for Aa SNP genotypes. A significant dominant model finding will only be valid when the additive model is also significant, otherwise overdominance is implied.

SOLAR employs a maximum likelihood algorithm to estimate the variance component parameters, and gives likelihood values for the general variance components model (Amos, 1994):

$$p = \mu + \sum \beta_i x_i + G + e,$$

where p is the phenotypic data, μ is the overall mean of the quantitative trait, β_i are the covariate regression coefficients, x_i the covariates, G is the random polygenic effect, and e the non-shared environmental effect or random error. Regression coefficients for genotype-specific means are assessed using a likelihood ratio test comparing the likelihood of a model in which the coefficient is estimated to the likelihood of the model in which it is constrained to zero. This linkage disequilibrium test is a conventional association approach, which tests for differences in the trait mean by genotype, taking into account the relatedness of the individuals, and is, therefore susceptible to false positives caused by population stratification. To curtail possible population stratification effects, linkage disequilibrium analysis was performed using the Caucasian-only subset of the available COGA dataset (1067 individuals from 210 families).

When evidence of both significant linkage and SNP linkage disequilibrium is observed, then linkage analysis can be re-run conditional on this measured genotype to evaluate whether the associated polymorphism can account for the observed linkage signal (Soria et al., 2000). If the associated polymorphism is the sole functional variant in the candidate gene then no evidence of linkage should remain in the conditional linkage analysis (i.e. LOD score drops to zero). Alternatively, if the genotyped variant is only in disequilibrium with the causative variant, or if it is one of several functional polymorphisms influencing the phenotype, then the LOD score in the conditional

analysis will be reduced but evidence for linkage will remain (Almasy and Blangero, 2003).

3. Results

Estimates of the ERO mean energy were calculated via the S-transform time-frequency algorithm (Stockwell et al., 1996) as described in Section 2. Data were extracted within a time-frequency region of interest (TFROI) corresponding to the P300 time window, and across the delta and theta frequency bands. The energy estimates were averaged across recording channels to form three scalp regions (frontal, central and parietal) as depicted in Fig. 1. The TFROI phenotypes were derived using both target (infrequent) and non-target (frequent) visual oddball data. Fig. 2 serves to illustrate the phenotype measure.

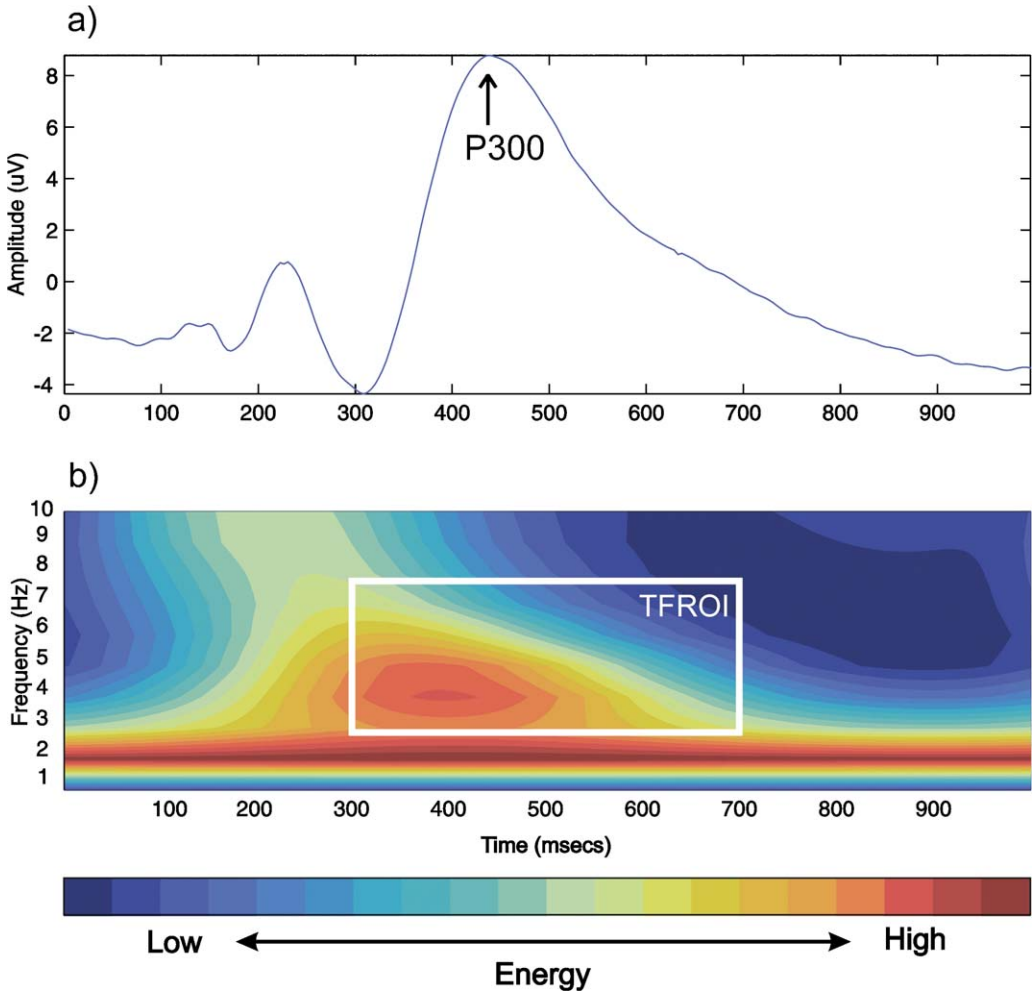

Fig. 2. (a) Plot of the target case visual grand mean evoked potential for ~1300 individuals of the COGA genotyped dataset (channel CZ). The P300 component is observed to occur between 300 and 700 ms, and is primarily constituted from delta and theta band energy. (b) Time-frequency representation of the target case visual evoked ERP energy distribution for channel CZ, calculated using the S-transform (see Section 2 for details). The S-transform distribution was calculated on each subject's individual trial data and averaged within each subject, then across each subject to create the grand averaged time-frequency distribution depicted in the figure. An example time-frequency region of interest (TFROI) is shown on the figure (white rectangle) for the P300 time window (300–700 ms) and the theta frequency band (3–7 Hz); mean values are calculated within the P300 time window and delta and theta frequency band TFROI windows for each subject and used as phenotypes in the genetic analysis.

Fig. 2a depicts grand averaged data across the entire dataset for the target case and the CZ channel. Fig. 2b is the corresponding grand mean S-transform time-frequency representation of the data. The mean TFROI value for each individual was utilized as the phenotype.

The initial genome-wide linkage scan of the theta band P300-window TFROI data revealed significant linkage (LOD=3.5) on chromosome 7 between the markers D7S1837 and D7S509 (at 171 cM) with the frontal grouping of electrodes (Fig. 3). The central and parietal electrode groups showed weaker but suggestive linkage with the same region (central LOD = 1.74 at 163 cM; parietal LOD = 1.86 at 163 cM). Subsequent re-analysis of the theta band phenotype using the Caucasian-only data subset established suggestive linkage (LOD = 2.6) at the same location (171 cM) for the frontal grouping of electrodes (Fig. 3). Central and parietal lead groupings again showed weaker but suggestive linkage (central LOD = 1.47 at 163 cM; parietal LOD = 1.97 at 163 cM). The reduced LOD peaks are likely to be due to the smaller sample size. Heritability estimates for the theta band evoked oscillations were comparable to estimates derived from P300 ERP amplitudes (Almasy et al., 1999) (frontal = 0.55, central = 0.54, parietal = 0.57). Chromosome

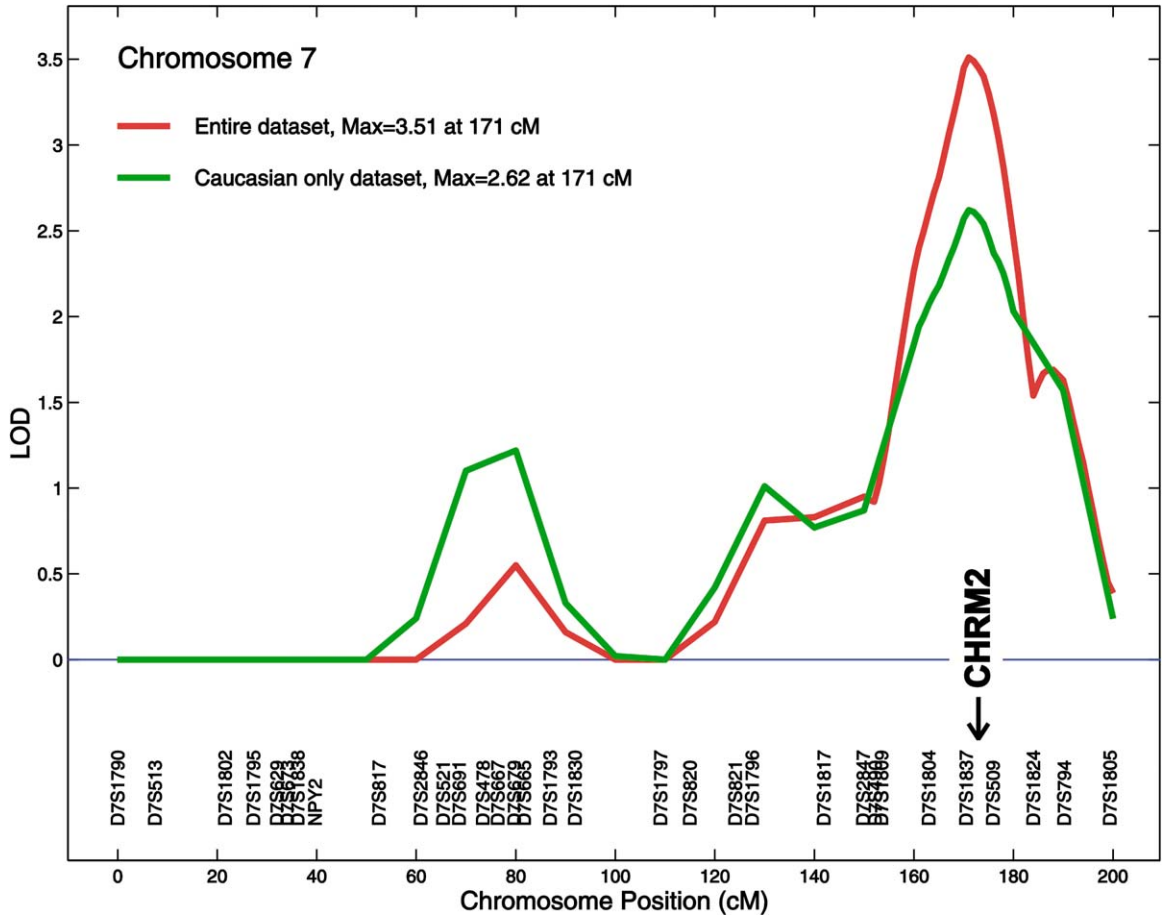

Fig. 3. Linkage result of the target case visual evoked oscillation phenotypic data (300–700 ms and theta band TFROI) on chromosome 7. Results are displayed for linkage evaluated with the entire genotyped COGA dataset (red curve) available with visual oddball data, and with the Caucasian-only subset (green curve). Maximum LOD scores for both linkage runs are situated near the location of the cholinergic muscarinic receptor gene *CHRM2*. The entire dataset consists of 1337 individuals from 253 families; the Caucasian-only dataset contains 1067 individuals from 210 families. The decreased LOD score peak for the Caucasian-only group is likely due to the reduced sample population.

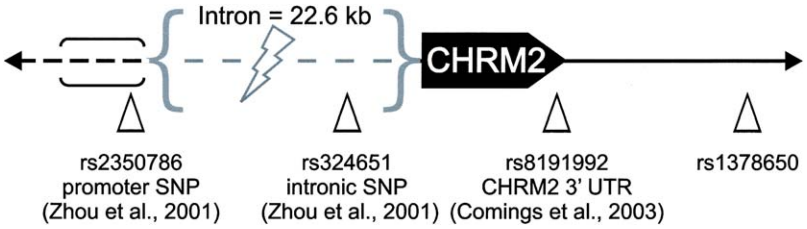

Fig. 4. Location of single nucleotide polymorphisms (SNPs) used in the LD analysis, within and flanking the *CHRM2* gene on chromosome 7.

7 LOD score curves for both the entire dataset and Caucasian-only subset are provided in Fig. 3.

The muscarinic cholinergic receptor gene *CHRM2* is within the 20 cM region of linkage. The muscarinic cholinergic receptors are G-protein coupled receptors that influence many effects of acetylcholine in the central and peripheral nervous system, and hence are expected to have a direct influence on P300 generation (Frodl-Bauch et al., 1999a). Also, the cholinergic muscarinic genes have a role in memory and cognition (Calabresi et al., 1998; Comings et al., 2003).

To test whether the observed theta band linkage findings were directly influenced by the *CHRM2* gene, four single nucleotide polymorphisms were genotyped in and around the candidate gene (rs2350786, rs324651, rs8191992 and rs1378650). Fig. 4 shows the location of these SNPs within the *CHRM2* gene structure. The rs8191992 SNP lies in the 3′ UTR and is encoded by the exon (Comings et al., 2003) while the other SNPs are within the genomic structure of *CHRM2*. Estimates of linkage disequilibrium quantified by Lewontin's D' (Lewontin, 1964) and delta^2 between the SNPs are given in Table 1a. Values of D' suggest that SNPs rs324651, rs8191992 and rs1378650 are in high LD (0.79–0.97) with each other, whereas rs2350786 shows only moderate LD with the other SNPs (0.44–0.67). We, therefore do not expect independent results from the three SNPs in high LD. Table 1b gives the *CHRM2* SNP genotype frequencies calculated using the entire phenotype dataset. Despite high LD between rs324651, rs8191992 and rs1378650, the SNP rs324651 shows markedly different allele frequencies, possibly caused by a recent mutation and reflected in the lower delta^2 value (since this measure includes allele variant frequencies). One of the rs324651 SNP homozygotes was rare (<2%) and so it was removed from further analysis.

Estimates of measured genotype linkage disequilibrium between the QTL and the remaining three *CHRM2* SNPs were obtained using techniques outlined in Section 2 for Caucasian-only theta and delta band P300 TFROI data (1067 individuals from 210 families). Additive model LD *P*-values for target case theta band frontal, central and parietal region phenotype data are outlined in Table 2. For this phenotype, the frontal and central regions show significance with the rs2350786 SNP (0.01), while the parietal region shows borderline significance with this SNP (0.04). The other SNPs (which are in high LD with each other) did not show additive model significance, while addition of a non-additive component did not improve the results. Since we observed moderate to high LOD scores for these phenotypes, linkage analysis was re-

Table 1a
Estimates of delta^2 (lower) and D' (upper) for *CHRM2* SNPs

delta^2\D'	rs2350786	rs324651	rs8191992	rs1378650
rs2350786	–	0.67	0.44	0.60
rs324651	0.028	–	0.97	0.83
rs8191992	0.13	0.089	–	0.79
rs1378650	0.23	0.068	0.6	–

D' values indicate that SNPs rs324651, rs8191992 and rs1378650 are in high LD (D': 0.79–0.97). The SNP rs2350786 shows moderate LD with the other SNPs (D': 0.44–0.67).

Table 1b
Measured genotype frequencies calculated from the entire COGA genotyped dataset

	AA	Aa	aa	Total
rs2350786	0.5 (659)	0.39 (517)	0.11 (151)	1327
rs324651	0.78 (1029)	0.2 (270)	0.02 (26)	1325
rs8191992	0.35 (469)	0.46 (610)	0.19 (247)	1326
rs1378650	0.34 (454)	0.47 (620)	0.19 (255)	1329

SNPs rs8191992 and rs1378650 have very similar genotype frequencies as expected from the high LD estimates.

Table 2
Linkage (indicated using LOD scores) and additive model measured genotype linkage disequilibrium results (indicated by additive model *P*-values) for the theta band P300 window target case ERO phenotype, using the Caucasian-only data subset (1067 individuals from 210 families)

Region	SNP	LOD score	LOD score with covariate	Percent decrease (%)	Additive model *P*-value
Frontal	rs2350786	2.62 (171 cM)	2.32	12	0.01*
	rs8191992		2.62	–	0.43
	rs1378650		2.62	–	0.14
Central	rs2350786	1.47 (163 cM)	1.32	10	0.01*
	rs8191992		1.47	–	0.41
	rs1378650		1.47	–	0.07
Parietal	rs2350786	1.97 (163 cM)	1.75	11	0.04*
	rs8191992		1.97	–	0.71
	rs1378650		1.97	–	0.22

Linkage disequilibrium analysis with additive model measured genotype data reveals significant association of the frontal and central region phenotype with SNP rs2350786. Linkage analysis conditional on the additive model measured genotype data results in approximately 10% decrease in frontal, central and parietal peak LOD scores with the same SNP. Due to non-independence between the phenotypes measures and between the SNP data, the presented *P*-values are not corrected for multiple testing. $*P<0.05$.

run conditional on the measured genotype (Almasy and Blangero, 2003). Inclusion of rs2350786 SNP additive model covariate produced an ~10% LOD score drop for frontal, central, and parietal theta band phenotypes (Table 2) suggesting that this SNP region plays some functional significance on the phenotype. However, since the effect size is small, and strong evidence for linkage remains, the rs2350786 SNP does not wholly account for the entire linkage signal. Separate linkage and linkage disequilibrium findings imply that the SNPs tested do not account for the entire linkage effect; however, the functional variants that influence the phenotype are likely to lie in or very near the *CHRM2* gene. No equivalent linkage or significant measured genotype findings were found for the corresponding non-target case data.

Table 3
Additive and dominant measured genotype linkage disequilibrium analysis results for the delta band P300 window ERO phenotype (indicated by additive and dominant model *P*-values), using the Caucasian-only data subset (1067 individuals from 210 families)

CHRM2 SNPs	Target Polygenic heritability – Frontal: 0.37 – Central: 0.38 – Parietal: 0.44			Non-target Polygenic heritability – Frontal: 0.16 – Central: 0.27 – Parietal: 0.28		
	Region	Additive model *P*-value	Dominant model *P*-value	Region	Additive model *P*-value	Dominant model *P*-value
rs2350786	Frontal	0.85	0.57	Frontal	0.78	0.19
	Central	0.09	0.28	Central	0.71	0.56
	Parietal	0.09	0.17	Parietal	0.83	0.91
rs8191992	Frontal	0.45	0.4	Frontal	0.08	0.55
	Central	<0.01**	0.35	Central	0.19	0.77
	Parietal	<0.001***	0.19	Parietal	0.44	0.79
rs1378650	Frontal	0.45	0.26	Frontal	0.08	0.18
	Central	<0.01**	0.3	Central	0.61	0.56
	Parietal	<0.01**	0.08	Parietal	0.81	0.82

Both target and non-target case results are given. Highly significant LD findings are observed for the central and parietal region target case phenotype with SNPs rs8191992 and rs1378650, which are also in high LD with each other. $**P<0.01$, $***P<0.001$.

The delta band P300 evoked oscillation phenotype showed weak linkage signals at the *CHRM2* gene location (170 cM) on chromosome 7 (LOD scores: frontal = 0.2; central = 0.42; parietal = 0.39). Measured genotype analysis with the three *CHRM2* SNPs, however, revealed highly significant additive model LD between the target case central and parietal region phenotypes and SNPs rs8191992 and rs1378650 (P-value < 0.001 for rs8191992, see Table 3). Since both of these SNPs are in high LD with each other ($D' = 0.79$, see Table 1a), we expect similar findings. The target case central and parietal delta band phenotypic data are also highly correlated ($\rho = 0.88$), therefore we also expect similar results for these phenotypes. Frontal to central and frontal to parietal correlations were more moderate ($\rho = 0.68$ and $\rho = 0.53$, respectively). Effectively, because of the high LD between the SNPs and high phenotypic data correlations, these data suggest one highly significant result between central–parietal evoked delta oscillations with rs8191992 and rs1378650 *CHRM2* SNPs. Addition of a dominance component to the measured genotype model did not improve the results. Fig. 5 shows the parietal phenotype data plotted against additive measured genotype model variants. A clear linear increase is observed for the evoked delta oscillation phenotype across the additive model genotypes. However, because we do not observe a strong linkage signal with the delta band phenotype we cannot entirely rule out the remote possibility that the LD signal is due to a population admixture within the Caucasian-only data subset. Non-target data did not demonstrate significant additive and dominant measured genotype model effects. The fact that we do not observe similar findings with the non-target data suggests that the *CHRM2* gene has a functional significance associated with cognitive processing of the target case in the visual oddball paradigm.

Heritability estimates derived from the target case delta phenotype (frontal: 0.37; central 0.38; parietal 0.44) were smaller in amplitude than the equivalent theta band heritability estimates (frontal: 0.54; central 0.55; parietal 0.54). The weak observed delta band linkage signal on chromosome 7 could be a reflection of this smaller phenotype heritability value and a consequent need for a larger dataset to attain greater statistical power. Heritability estimates calculated from the non-target case delta band phenotype (frontal: 0.16; central 0.27; parietal 0.28) are markedly reduced from the target case estimates; these heritability values are compatible with the case-specific nature of visual evoked delta oscillations. Similar case-dependent heritability findings have been reported for P300 component amplitudes (Almasy et al., 1999), in which target amplitude estimates (PZ channel: 0.51) are larger than non-target case (PZ channel: 0.32) and novel case (PZ channel: 0.32).

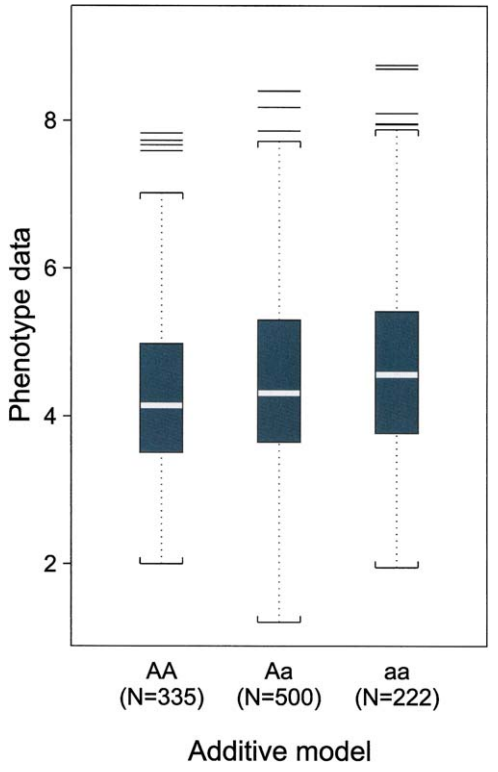

Fig. 5. Boxplot of the target case visual evoked delta band parietal region phenotypes plotted against additive measured genotypes derived from rs8191992 SNP data. Individuals included in the LD analysis have been restricted to the Caucasian-only subset. The electrophysiological phenotype is observed to vary linearly with the additive model genotypes; consequently, no dominant model effect is present. The boxplot horizontal white line depicts the median response, the bottom and top of the box shows the 25 and 75 percentiles, respectively, (interquartile range), while the box whiskers indicate 1.5 times the interquartile range of the data. Points lying outside the boxplot whiskers are represented by horizontal lines; these points could be inferred as outliers.

4. Discussion

Recent work has revealed that the time-course of the ERP N200 and P300 components are comprised chiefly of oscillations in the delta and theta frequency range (Stampfer and Basar, 1985; Demilrap et al., 1999). Delta oscillations primarily underlie the P300 component, whereas theta oscillations are involved in both the P300 and earlier N200 components. These evoked delta and theta oscillations may occur either as amplitude modulated fixed-latency events or as a result of sensory-induced phase modulation of ongoing dynamic brain activity. Indeed, some researchers now regard basic neuroelectric processing as being constituted from event-related oscillations rather the event-related potentials (Karakas et al., 2000a,b), although it is likely a combination of both (Makeig et al., 2002). The P300 is therefore considered to be built-up of delta and theta oscillations superimposed at approximately 60% to 40% proportions, respectively, with the explanatory power of the delta component higher at posterior sites, and a larger proportion of the theta component being fronto-central (Karakas et al., 2000b). The source generators of these P300 oscillation components are expected to be similar to those suggested for the P300 ERP. The delta component of the P300 is understood to be generated by cortico–cortical interactions (Devrim et al., 1999) with the likely influence of sub-cortical structures, while the theta component has been related to cortico–hippocampal and fronto–limbic interactions (Miller, 1985; Karakas et al., 2000a).

Studies of event-related oscillation data suggest that cognitive functions are represented by integration of parallel multi-frequency evoked oscillations, and that evoked oscillations are valid indexes of cognition (Karakas et al., 2000a; Herrmann and Knight, 2001). For this reason event-related oscillation data were adopted in this study as phenotypic data for genetic analyses of cognitive processes as opposed to the more traditional P300 ERP amplitude measures. Additionally, recent results from a study of the genetic correlation between P300 amplitudes and EEG power spectrum indicate that a proportion of the genetic influence on the P300 amplitude is explained by the heritability of slow EEG rhythms (Anokhin et al., 2001). The authors of the study suggest that the results agree well with the recent view that the low frequency components of ERP's are generated by stimulus-induced synchronization of ongoing EEG oscillations (Klimesch et al., 2001). In order to distinguish genetic relationships between the P300 amplitude and cognition, it is suggested that EEG characteristics need to be included as covariates with genetic analyses concerned with inter-individual ERP amplitude differences (Anokhin et al., 2001). In this study, we have taken an alternative approach. By employing event-related oscillation phenotypes derived from time-frequency representations of individual trial data, we are able to include background non-phase locked evoked activity with the phase-locked stimulus-induced activity in the phenotype measure. Locus-specific genetic effect differences observed between infrequent (target condition) and frequent (non-target condition) are then reliably attributed to cognitive processing specific to one of the conditions.

The genetic underpinnings of evoked potentials, and underlying evoked oscillations, are likely to stem from regulatory genes which control the neurochemical processes of the brain, and therefore influence neural function. Excitatory and inhibitory post-synaptic potentials (EPSP's and IPSP's) triggered by neurotransmitters contribute to the formation of evoked potentials. The major neurochemical substrates, which are thought to contribute to the P300 wave are the glutamatergic (excitatory), GABAergic (inhibitory) and cholinergic systems (Frodl-Bauch et al., 1999a). The dopaminergic, serotonergic and adrenergic systems are deemed to have less of an important role and more of an indirect influence on the P300 wave. Glutamatergic neurotransmission is therefore directly responsible for the generation of EPSP's. Acetylcholine and GABA then modulate these EPSP's with GABA reducing and acetylcholine enhancing evoked amplitudes.

The function of acetylcholine in the cortex has been attributed to the discriminatory process, to the efficiency of processing sensory and association information, and to stimulus significance evaluation (Perry et al., 1999). Basal forebrain cholinergic neurons project to the cortex and to the thalamic nucleus, which includes the reticular nucleus—an area associated with selective attention (Mitrofanis and Guillery, 1993). Acetylcholine has been demonstrated to be involved in P300 generation (Callaway, 1983). Administration of cholinergic agonists (e.g. carabachol)

and antagonists (e.g. scopolamine) have demonstrated modified memory performance, and modified P300 amplitude and latencies in humans (Mohs and Davies, 1985; Hammond et al., 1987; Meador et al., 1987; Potter et al., 2000). Animal studies also indicate a strong influence of the cholinergic system on P300 characteristics. For example, lesions of the septal cholinergic system in cats resulted in significantly reduced P300-like amplitudes (Harrison et al., 1988). Administration of muscarinic agonists in macaques led to enlarged auditory P300-like amplitudes (O'Neill et al., 2000). Visual discrimination and P300 amplitudes have been observed to be affected by cholinergic muscarinic agents in monkeys (Antal et al., 1994).

In vitro studies of the rat have suggested that the presence of a cholinergic agonist in the rat hippocampus induces oscillations in the delta, theta and gamma frequency range (Fellous and Sejnowski, 2000; Tiesinga et al., 2001). Slow (theta band) neocortical oscillations have been induced in rat neocortical slices by use of cholinergic agonists (Lukatch and MacIver, 1997). Results from these studies fit the pharmacological and physiological model of an ascending cholinergic pathway, originating in the brain stem, which modulates oscillations. These slow hippocampal and neocortical oscillations are likely to be implicated with arousal, sensory/motor processing, learning and memory.

In vitro administration of moderate amounts of the muscarinic agonist carbachol in the rat hippocampus induced synchronized delta oscillations, whereas higher concentrations produced short episodes of theta oscillations (Fellous and Sejnowski, 2000). Carbachol-induced delta rhythms were not observed concurrent with carbachol-theta. It is interesting to note that our theta and delta band phenotypes did not provide associations with the same *CHRM2* SNPs. These data may imply that the theta and delta systems are distinct. Indeed, the different region-wise dependency of the associations (frontal for theta vs. parietal for delta) offers credence to the notion of different event-related oscillatory mechanisms. In addition, the grand mean energy curves indicate that theta band distribution peaks approximately 100 ms prior to the delta band distribution peak (approx. 350 ms and 450 ms, respectively). Comparable with concentration dependent carabachol-induced oscillations previously described (Fellous and Sejnowski, 2000), this observation may imply that early theta band oscillations are evoked by high concentrations of muscarinic activity. Delta band oscillations then result from later reduced muscarinic activity.

Studies on M1 cholinergic muscarinic receptor mutant mice suggest cortical memory dysfunction or impaired hippocampal–cortical interaction, that is specific to working memory (Anagnostaras et al., 2003) and hence possibly related to the human P300. M2 cholinergic muscarinic receptor gene (*CHRM2*) SNPs have been demonstrated to show association with diagnosis of depression in woman (Comings et al., 2002) and measures of IQ and years of education with parents of twins from the Minnesota Twin and Family Study (Comings et al., 2003). Taken together with the results presented here, these studies strongly support the idea that cholinergic pathways are important for cognition and memory. As with all genetic studies of complex phenotypes caution must be advised until these results are supported and replicated with alternate datasets. Converging lines of evidence, however, indicate that cholinergic receptor genes have a functional role in human cognition via modulation of the neuroelectric oscillations.

Acknowledgements

The Collaborative Study on the Genetics of Alcoholism (COGA) (Principal Investigator: H. Begleiter; Co-Principal Investigators: L. Bierut, H. Edenberg, V. Hesselbrock, Bernice Porjesz) includes nine different centers where data collection, analysis, and storage take place. The nine sites and Principal Investigators and Co-Investigators are: University of Connecticut (V. Hesselbrock); Indiana University (H. Edenberg, J. Nurnberger Jr., P.M. Conneally, T. Foroud); University of Iowa (R. Crowe, S. Kuperman); SUNY HSCB (B. Porjesz, H. Begleiter); Washington University in St. Louis (L. Bierut, J. Rice, A. Goate); University of California at San Diego (M. Schuckit); Howard University (R. Taylor); Rutgers University (J. Tischfield); Southwest Foundation (L. Almasy). Lisa Neuhold serves as the NIAAA Staff Collaborator. This national collaborative study is supported by the NIH Grant U10AA08403 from the

National Institute on Alcohol Abuse and Alcoholism (NIAAA).

In memory of Theodore Reich, M.D., Co-Principal Investigator of COGA since its inception and one of the founders of modern psychiatric genetics, we acknowledge his immeasurable and fundamental scientific contributions to COGA and the field.

References

Almasy, L., Blangero, J., 1998. Multipoint quantitative-trait linkage analysis in general pedigrees. Am. J. Hum. Genet. 62, 1198–1211.

Almasy, L., and Blangero, J., 2003. Exploring positional candidate genes: linkage conditional on measured genotype (in press).

Almasy, L., Porjesz, B., Blangero, J., Begleiter, H., Chorlian, D.B., O'Connor, S.J., et al., 1999. Heritability of event-related brain potentials in families with a history of alcoholism. Neuropsychiatr. Genet. 88, 383–390.

Amos, C.I., 1994. Robust variance-components approach for assessing genetic linkage in pedigrees. Am. J. Hum. Genet. 54, 535–543.

Anagnostaras, S.G., Murphy, G.G., Hamilton, S.E., Mitchell, S.L., Rahnama, N.P., Nathanson, N.M., et al., 2003. Selective cognitive dysfunction in acetylcholine M1 muscarinic receptor mutant mice. Nat. Neurosci. 6, 51–58.

Anokhin, A.P., Van Baal, G.C., Van Beijsterveldt, C.E., de Geus, E.J., Grant, J., Boomsma, D.I., 2001. Genetic correlation between the P300 event-related brain potential and the EEG power spectrum. Behav. Genet. 31, 545–554.

Antal, A., Kovanecz, I., Bodis-Wollner, I., 1994. Visual discrimination and P300 are affected in parallel by cholinergic agents in the behaving monkey. Physiol. Behav. 56, 161–166.

Basar, E., 1980. EEG-Brain Dynamics: Relation Between EEG and Brain Evoked Potentials. Elsevier, New York.

Basar, E., Basar-Eroglu, C., Karakas, S., Schurmann, M., 1999. Are cognitive processes manifested in event-related gamma, alpha, theta and delta oscillations in the EEG? Neurosci. Lett. 259, 165–168.

Basar, E., Basar-Eroglu, C., Karakas, S., Schurmann, M., 2000. Brain oscillations in perception and memory. Int. J. Psychophysiol. 35, 95–124.

Basar, E., Basar-Eroglu, C., Karakas, S., Schurmann, M., 2001. Gamma, alpha, delta, and theta oscillations govern cognitive processes. Int. J. Psychophysiol. 39, 241–248.

Begleiter, H., Reich, T., Hesselbrock, V.M., Porjesz, B., Li, T.K., Schuckit, M.A., et al., 1995. The Collaborative Study on the Genetics of Alcoholism. Alcohol Health Res. World 19, 228–236.

Begleiter, H., Porjesz, B., Reich, T., Edenberg, H.J., Goate, A., Blangero, J., et al., 1998. Quantitative trait loci analysis of human event-related brain potentials: P3 voltage. Electroencephalogr. Clin. Neurophysiol. 108, 244–250.

Blangero, J., Williams, J.T., Almasy, L., 2001. Variance component methods for detecting complex trait loci. Adv. Genet. 42, 151–181.

Boerwinkle, E., Chakraborty, R., Sing, C.F., 1986. The use of measured genotype information in the analysis of quantitative phenotypes in man. I. Models and analytical methods. Ann. Hum. Genet. 50, 181–194.

Calabresi, P., Centonze, D., Gubellini, P., Pisani, A., Bernardi, G., 1998. Blockade of M2-like muscarinic receptors enhances long-term potentiation at corticostriatal synapses. Eur. J. Neurosci. 10, 3020–3023.

Callaway, E., 1983. The pharmacology of human information processing. Psychopharmacologia 20, 359–370.

Cohen, H.L., Wang, W., Porjesz, B., Bauer, B.O., Kuperman, S., O'Connor, S.J., et al., 1994. Visual P300: an interlaboratory consistency study. Alcohol 11, 583–587.

Comings, D.E., Wu, S., Rostamkhani, M., McGue, M., Lacono, W.G., MacMurray, J.P., 2002. Association of the muscarinic cholinergic 2 receptor gene with major depression in woman. Am. J. Med. Genet. 114, 527–529.

Comings, D.E., Wu, S., Rostamkhani, M., McGue, M., Lacono, W.G., Cheng, L.S.-C., et al., 2003. Role of cholinergic muscarinic 2 receptor (*CHRM2*) gene in cognition. Mol. Psychiatr. 8, 10–13.

Demilrap, T., Ademoglu, A., Schurmann, M., Basar-Eroglu, C., Basar, E., 1999. Detection of P300 waves in single trials by the wavelet transform (WT). Brain Lang. 66, 108–128.

Devrim, M., Demiralp, T., Ademoglu, A., Kurt, A., 1999. A model for P300 generation based on responses to near-threshold visual stimuli. Cognit. Brain Res. 8, 37–43.

Donchin, E., 1979. Event-related brain potentials: A tool in the study of human information processing. In: H. Begleiter (Ed.), Evoked Brain Potentials and Behavior, Plenum, New York, pp. 13–88.

Donchin, E., Coles, M.G.H., 1988. Is the P300 component a manifestation of context updating? Behav. Brain Sci. 11, 357–374.

Doppelmayr, M., Klimesch, W., Schwaiger, J., Auinger, P., Winkler, T., 1998. Theta synchronization in the human EEG and episodic retrieval. Neurosci. Lett. 257, 41–44.

Fellous, J.-M., Sejnowski, T., 2000. Cholinergic induction of oscillations in the hippocampal slice in the slow (0.5–2 Hz), theta (5–12 Hz) and gamma (35–70 Hz) bands. Hippocampus 10, 187–197.

Frodl-Bauch, T., Bottlender, R., Hegerl, U., 1999a. Neurochemical substrates and neuranatomical generators of the event-related P300. Neuropsychobiology 40, 86–94.

Frodl-Bauch, T., Gallinat, J., Meisenzahl, E.M., Moller, H.J., Hegerl, U., 1999b. P300 subcomponents reflect different aspects of psychopathology in schizophrenia. Biol. Psychiatr. 45, 116–126.

Gabor, D., 1946. Theory of communications. J. Inst. Electr. Eng. 93, 429–457.

Geffen, G., Wright, M., Green, H., Gillespie, N., Smyth, D., Evens, D., et al., 1997. Effects of memoryload and distraction on performance and event-related slow potentials in a visuaospatial working memory task. J. Cognit. Neurosci. 9, 743–757.

Ghosh, S., Begleiter, H., Porjesz, B., Edenberg, H., Foroud, T.,

Reich, T., 2003. Linkage mapping of beta 2 EEG waves via non-parametric regression. Am. J. Med. Genet. B 118, 66–71.

Halgren, E., Squires, N.K., Wilson, C.L., Rohrbaugh, J.W., Babb, T.L., Crandall, P.H., 1980. Endogenous potentials generated in the human hippocampal formation and amygdala by infrequent events. Science 210, 803–805.

Hammond, E.J., Meador, K.J., Aung-Din, R., Wilder, B.J., 1987. Cholinergic modulation of human P3 event-related potentials. Neurology 37, 346–350.

Harrison, J.B., Buchwald, J.S., Kaga, K., Woolf, N.J., Butcher, L.L., 1988. 'Cat P300' disappears after septal lesions. Electroencephalogr. Clin. Neurophysiol. 69, 55–64.

Herrmann, C.S., Knight, R.T., 2001. Mechanisms of human attention: event-related potentials and oscillations. Neurosci. Biobehav. Rev. 25, 465–476.

Hruby, T., Marsalek, P., 2003. Event-related potentials—the P3 wave. Acta Neurobiol. Exp. 63, 55–63.

Karakas, S., Erzengin, O.U., Basar, E., 2000a. The genesis of human event-related responses explained through the theory of oscillatory neural assemblies. Neurosci. Lett. 285, 45–48.

Karakas, S., Erzengin, O.U., Basar, E., 2000b. A new strategy involving multiple cognitive paradigms demonstrates that ERP components are determined by superposition of oscillatory responses. Clin. Neurophysiol. 111, 1719–1732.

Katsanis, J., Jacono, W.G., McGue, M.K., Carlson, S.R., 1997. P300 event-related potential heritability in monozygotic and dizygotic twins. Psychophysiology 34, 47–58.

Klimesch, W., Doppelmayr, M., Pachinger, T., Ripper, B., 1997. Brain oscillations and human memory performance: EEG correlates in the upper alpha and theta band. Neurosci. Lett. 238, 9–12.

Klimesch, W., Doppelmayr, M., Yonelinas, A., Kroll, N., Lazzara, M., Rohm, D., et al., 2001. Theta synchronization during episodic retrieval: neural correlates of conscious awareness. Cognit. Brain Res. 12, 33–38.

Lachaux, J.P., Chavez, M., Lutz, A., 2003. A simple measure of correlation across time, frequency and space between continuous brain signals. J. Neurosci. Meth. 123, 175–188.

Lewontin, R.C., 1964. The interaction of selection and linkage disequilibrium. Genetics 49, 49–67.

Lukatch, H.S., MacIver, M.B., 1997. Physiology, pharmacology, and topography of cholinergic neocortical oscillations in vitro. J. Neurophysiol. 77, 2427–2445.

Makeig, S., Westerfield, M., Jung, T.P., Enghoff, S., Townsend, J., Courchesne, E., et al., 2002. Dynamic brain sources of visual evoked responses. Science 295, 690–694.

Mangun, G.R., Buonocore, M.H., Girelli, M., Jha, A.P., 1998. ERP and fMRI measures of visual spatial selective attention. Human Brain Mapp. 6, 383–389.

Meador, K.J., Loring, D.W., Adams, R.J., Platel, B.R., Davis, H.C., Hammond, E.J., 1987. Central cholinergic systems and auditory P3 evoked potential. Int. J. Neurosci. 33, 199–205.

Miller, R., 1985. Cortico–Hippocampal Interplay and the Representation of Contexts in the Brain Springer, Berlin.

Mitrofanis, J., Guillery, R.W., 1993. New views of the thalamic reticular nucleus in the adult and in the developing brain. Trends Neurosci. 16, 240–245.

Mohs, R.C., Davies, K.L., 1985. Interaction of choline and scopalamine in human memory. Life Sci. 37, 193–197.

O'Connor, S.J., Morzorati, S., Christian, J.C., Li, T.K., 1994. Heritable features of the auditory oddball event-related potential: peaks, latencies, morphology and topography. Electroencephalogr. Clin. Neurophysiol. 92, 115–125.

Okada, Y.C., Kaufman, L., Williamsen, S.J., 1983. The hippocampal formation as a source of slow endogenous potentials. Electroencephalogr. Clin. Neurophysiol. 55, 417–426.

O'Neill, J., Halgren, E., Marinkovic, K., Siembieda, D., Refai, D., Fitten, L.J., et al., 2000. Effects of muscarinic and adrenergic agonism on auditory P300 in the macaque. Physiol. Behav. 70, 163–170.

Perry, E., Walker, M., Grace, J., Perry, R., 1999. Acetylcholine in mind: a neurotransmitter correlate of consciousness? Trends Neurosci. 22, 273–280.

Polich, J., Kok, A., 1995. Cognitive and biological determinants of P300: an integrative review. Biol. Psychol. 41, 104–146.

Porjesz, B., Almasy, L., Edenberg, H., Wang, K., Chorlian, D.B., Foroud, T., et al., 2002. Linkage disequilibrium between the beta frequency of the human EEG and a GABA(A) receptor gene locus. PNAS 99, 3729–3733.

Potter, D.D., Pickles, C.D., Roberts, R.C., Rugg, M.D., 2000. Scopolamine impairs memory performance and reduces frontal but not parietal visual P3 amplitude. Biol. Psychol. 52, 37–52.

Rangaswamy, M., Porjesz, B., Chorlian, D.B., Wang, K., Jones, K.A., Bauer, L.O., et al., 2002. Beta power in the EEG of alcoholics. Biol. Psychiatr. 51, 831–842.

Rangaswamy, M., Porjesz, B., Chorlian, D.B., Wang, K., Jones, K.A., Bauer, L.O., Kuperman, S., O'Connor, S., Rohrbaugh, J., Reich, T., and Begleiter, H., 2004. Resting EEG in offspring of male alcoholics: beta frequencies. Int. J. Psychophysiol. (In press).

Rogers, R.L., Basile, L.F.H., Papanicolaou, A.C., Eisenberg, H.M., 1993. Magnetoencephalography reveals two distinct sources associated with late positive evoked potentials during visual oddball task. Cereb. Cortex 3, 163–169.

Roth, W.T., Pfefferbaum, A., Kelly, A.F., Berger, P.A., Kopel, B.S., 1981. Auditory event-related potentials in schizophrenia and depression. Psychiatr. Res. 4, 199–212.

Ruchkin, D.S., Canoune, H.L., Johnson, R., Ritter, O., 1995. Working memory and preparation elicit different patterns of slow wave event-related brain potentials. Psychophysiology 32, 399–410.

Schurmann, M., Basar-Eroglu, C., Kolev, V., Basar, E., 1995. A new metric for analyzing single-trial event-related potentials (ERPs) application to human visual P300 delta response. Neurosci. Lett. 197, 167–170.

Schurmann, M., Basar-Eroglu, C., Basar, E., 1997. Gamma responses in the EEG: elementary signals with multiple functional correlates. Neuroreport 8, 531–534.

Schurmann, M., Basar-Eroglu, C., Kolev, V., Basar, E., 2001. Delta responses and cognitive processing: single trial evaluations of human visual P300. Int. J. Psychophysiol. 39, 229–239.

Soria, J.M., Almasy, L., Souto, J.C., Tirado, I., Borell, M., Mateo,

V., et al., 2000. Linkage analysis demonstrates that the prothrombin G20210A mutation jointly influences plasma prothrombin levels and risk of thrombosis. Blood 95, 2780–2785.

Stampfer, H.G., Basar, E., 1985. Does frequency analysis lead to better understanding of human event-related potentials? Int. J. Neurosci. 26, 181–196.

Stockwell, R.G., Mansinha, L., Lowe, R.P., 1996. Localization of the complex spectrum: the S-transform. IEEE Trans. Signal Process. 44, 998–1001.

Sutton, S., Barren, M., Zubin, J., John, E.R., 1965. Evoked potential correlates of stimulus uncertainty. Science 150, 1187–1188.

Tiesinga, P.H.E., Fellous, J.-M., Jose, J.V., Sejnowski, T.J., 2001. Computational model of carbachol-induced delta, theta, and gamma oscillations in the Hippocampus. Hippocampus 11, 251–274.

Van Beijsterveldt, C.E.M., Molenaar, P.C.M., de Geus, E.J.C., Boomsma, D.I., 1998. Individual differences in P300 amplitude: a genetic study in adolescent twins. Biol. Psychol. 47, 97–120.

Van Beijsterveldt, C.E.M., Van Baal, G.C.M., 2002. Twin and family studies of the human electroencephalogram: a review and a meta-analysis. Biol. Psychol. 61, 111–138.

Yordanova, A., Kolev, V., 1998. Event-related alpha oscillations are functionally associated with P300 during information processing. Neuroreport 9, 3159–3164.